MICROSTRUCTURAL ASPECTS OF COLD FORMING PROCESSES IN PRECISION TUBE DRAWING

Martin Ridzoň[1,2], Milan Mojžiš[1,2], Lucia Domovcová[1,3], Jozef Bílik[2], Ľudovít Parilák[1,4]

[1]*ŽP Research and Development Centre, Kolkáreň 35, 976 81 Podbrezová, ridzon.m@zelpo.sk*

[2]*Faculty of Materials Science and Technology STU in Bratislava, Paulínska 16, 917 24 Trnava*

[3]Technical University of Košice, Department of Material Science, Faculty of Metallurgy, Slovakia

[4]*Technical University in Košice, Faculty of Manufacturing Technologies with a seat in Prešov, Department of Manufacturing Technologies, Prešov, Slovakia*

Abstract

The production of precision seamless steel tubes in Železiarne Podbrezová requires a detailed microstructural analysis of plastic deformation during cold forming on draw benches. Speaking of microstructural analysis we actually mean the impact of plastic deformation on the microstructure of the tube. For this, a detailed study of deformation and dislocation interaction mechanism during cold forming is necessary.

In this paper we present the microstructural analysis of selected material states focusing on the grain size of ferrite and the volumetric content of pearlite. The yield stress strengthening contribution has been estimated using additive law and the deformation strengthening contribution after the normalizing has been estimated using the law of geometrically necessary dislocations, allowing us to compare both contributions – grain strengthening R_z and dislocation strengthening R_D, respectively.

Keywords: cold forming, ferrite grain size, additive law

1. INTRODUCTION

In Železiarne Podbrezová, precision seamless steel tubes are being produced via multiple drawing operations, accompanied by additional operations such as pointing, pickling, lubrication, and heat treatment. From economic as well as manufacturing point of view, the whole production process depends on various process parameters, for example the number of drawing passes and the type of heat treatment, respectively. The focus point of our experiment was the plastic deformation in all three drawing passes with the subsequent analysis of deformation textures of the microstructure. Plastic deformation in general has a clear impact on the state of the microstructure, rendering significant changes in ferritic grain geometry. This allows us to define the microplastic deformation in different locations of the material. At the substructure level of plastic deformation the movement of line dislocations takes place, caused by external stress state. The intensity of plastic deformation guarantees also the maneuverability of dislocations related to Von Mises criterion for five independent slip planes in the crystallographic structure, which ferritic steel with K8 lattice (BCC) satisfies, even at room temperature.

2. MATERIAL AND EXPERIMENTAL METHODS

For the experiment, 30 hot rolled tubes with dimension 33,7 x 2,6 mm made of E235 ferritic-pearlitic steel grade (Tab. 1) were selected. The tubes were normalized at 900 ºC and cut to lengths of 4,5 m.

Mechanical properties according to EN 411 353

$R_{e,min}$ = 235 MPa, $R_{m,min}$ = 343 MPa, $R_{m,max}$ = 441 MPa, A_5 = 25 %

Tab. 1 Chemical composition of E235 steel grade (EN 411353)

	C	Mn	Si	P	S		B	Nb	Ti	W	As
min	0,070	0,40	0,17	-	-	min	-	-	-	-	-
max	0,090	0,50	0,25	0,015	0,015	max	0,0030	0,010	0,010	0,03	0,020
	0,076	0,42	0,20	0,008	0,012		0,0003	0,002	0,002	0,00	0,006
	Cu	Cr	Ni	Al	Cu		Zn	Sb	Fe	Ce	Co
min	-	-	-	0,020	-	min	-	-	-	-	-
max	0,25	0,10	0,15	0,030	0,25	max	-	0,008	-	-	-
	0,17	0,05	0,07	0,023	0,17		0,003	0,002	98,91	0,001	0,0070
	AlSo	Sn	Ca	N	Pb						
min	-	-	-	-	-						
max	-	0,020	-	0,0090	0,005						
	0,018	0,014	0,0021	0,0090	0,001						

3. TECHNOLOGY OF TUBE COLD DRAWING

Our aim was to draw the hot rolled tube of dimension 33,7 x 2,6 mm into 18,0 x 1,5 mm. For this, the drawing technology with a fixed cylindrical plug was selected. The deformation (reduction) values for individual drawing passes can be seen in Tab 2.

Fig. 1 Tube drawing example using plug drawing technology [3]

All experimental tubes were continuously sampled for the next experimental program that is presented in Tab 3.

Table 2 Dimensions and reductions (three-pass technology)

Draw No.	Input dimension			Output dimension			Reduction
	O.D.	W.T.	lenght	O.D.	W.T.	L	r
1	33,7	2,6	4000	28	2,15	**5558**	**31,27**
2	28	2,15	5558	22,85	1,725	**8202**	**34,43**
3	22,85	1,725	8202	18	1,475	**11993**	**33,11**

O.D. – outer diameter, W.T. – wall thickness, L – length

NZ – normalized (heat treated)

Tab. 3 Samples according to experimental program

No.	Outer diameter O.D. [mm]	Wall thickness W.T [mm]	Condition
A1	33,70	2,600	Rolled
A2	33,70	2,600	Rolled + NZ
ZB	28,00	2,150	1st draw
ZB3	28,00	2,150	1st draw + NZ
ZC	22,85	1,725	2nd draw
ZC3	22,85	1,725	2nd draw + NZ
ZD	18,00	1,475	3rd draw
ZD3	18,00	1,475	3rd draw + NZ

4. MICROSTRUCTURAL ANALYSIS

For selected structural conditions microstructural analyses were made, focusing on the grain size of the ferrite and volume of the pearlite. For yield stress strengthening we used additive law [4] and for the deformation strengthening after normalization we used the law of geometrically necessary dislocations. This law allows us to compare the contribution of the grain size of ferrite – grain strengthening R_z with the contribution of geometrically necessary dislocations (dislocation strengthening R_D) as follows:

$$R_z = k_y . d^{-\frac{1}{2}} \quad (1) \qquad R_D = \alpha . G . b . \sqrt{\rho} \quad (2)$$

Where:

k_y = 15 N.mm$^{-3/2}$ – ferritic grain boundary barrier effect against dislocation motion

d = 6 μm = 6.10^{-3}mm – average ferritic grain size,

α = 0,33 – strength of dislocation net, G = 81 000 MPa (shear modulus),

b = 2,5 10^{-10} m – magnitude of Burgers dislocation vector, ρ x 10^{-9} [cm^{-2}] – dislocation density

Then we can write:

$$R_z = R_D \quad (3) \qquad k_y . d^{-\frac{1}{2}} = \alpha . G . b . \sqrt{\rho} \quad (4)$$

After normalizing we determined the average ferritic grain size (6 microns) along with the pearlitic volume fraction (5,3 %). The microstructure in Fig. 2 is a ferritic-pearlitic one and fairly homogeneous (Fig. 2a). Pearlitic grains are located mainly at the boundaries of smaller ferritic grains (Fig. 2b). [1].

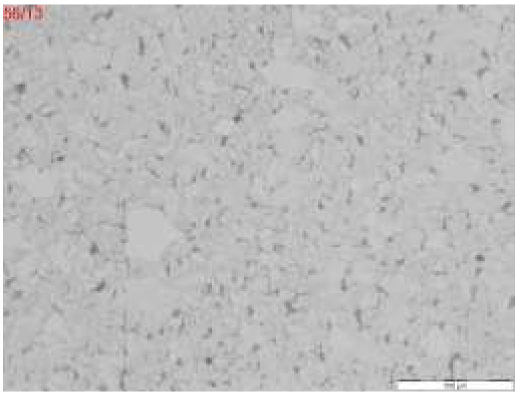

a)

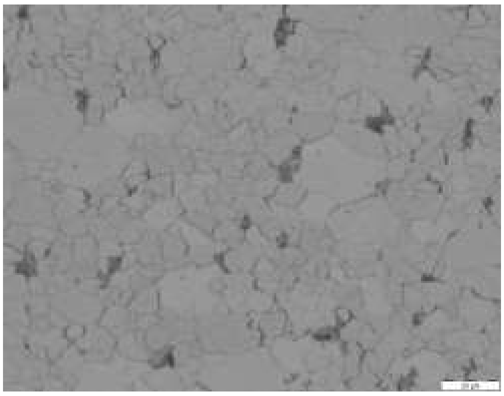

b)

Fig. 2 Steel grade E235 after rolling and normalizing: magnification 100 μm (a) and 20 μm (b))

According to (1) – (4) and estimated ferritic grain size we calculated the so called geometrically necessary dislocations density as follows:

Calculation of dislocation density after normalizing:

$$\rho = \frac{1}{d} . \left(\frac{k_y}{\alpha . G . b} \right)^2 \quad (5) \qquad \rho_{po\,N\check{Z}} = 8{,}4 \, . 10^8 cm^{-2} \quad (6)$$

The dislocation density relates (in the order of magnitude) to the microstructure while the contribution of dislocation strengthening can be calculated according (2), using (8).

The yield stress after normalization R_e = 285 MPa. Using the additive law for the yield stress [2] for given chemical composition and given microstructure we can estimate the contribution of pearlite strengthening R_{PR} = 16 MPa, the manganese substitution strengthening R_{Mn} = 21 MPa, and the silicon substitution strengthening R_{Si} = 17 MPa. Then we obtain the real interstition strengthening contribution R_{INT} and internal lattice stress R_{PN}, so we can write R_{INT} + R_{PN} = 47 MPa (other authors claim 40 MPa).

Dislocation strengthening: $R_{D_{po\ N\check{Z}}} = \alpha . G . b . \sqrt{\rho}$ (7) $R_{D_{po\ N\check{Z}}} = 194\ MPa$ (8)

Next, we focused on the yield stress as the function of the number of drawing passes. We were following the theory which states that the increase in the yield stress is related to the deformation strengthening, which is in fact determined by dislocation strengthening that what is caused by increased dislocation density during cold forming.

Mechanical properties and dislocation functions

Estimation of mechanical properties, dislocation density, and dislocation strengthening for all investigated material conditions can be seen in Tab. 4 and 5, respectively.

Table 4 Mechanical properties

Sample	O.D. (mm)	W.T. (mm)	Condition	$R_{p\,0,2}$ (MPa)	R_m (MPa)	$A_{5,6}$ (%)	ε_{rov}
A1	33,7	2,6	Rolled	338	406	45,9	17,86
A2	33,7	2,6	Rolled + normalized	285	391	41,1	18,02
ZB	28	2,15	1st pass	593	614	9,7	1,27
ZC	22,85	1,725	2nd pass	704	706	7,2	0,31
ZD	18	1,475	3rd pass	728	732	5,8	0,38

Table 5 gives the calculated dislocation strengthening and dislocation density for each deformation state.

Table 5 Dislocation hardening and dislocation density

Condition	ρ x10^9 [cm^{-2}]	R_D [MPa]
Normalized	0,8	194
1st pass	5,8	502
2nd pass	8,6	613
3rd pass	9,3	637

Estimated dislocation densities are pretty realistic for current deformed state. Here, two things must be stressed out: during cold forming, different stress levels are emerging in the material, causing increased dislocation densities after each pass. The deformation capacity of the material in all three passes is not saturated but there is a significant increase of drawing forces after each subsequent pass.

Conditions after normalizing

After each pass we applied normalizing at 910 °C with 30 min soaking time, as seen in Tab 6. Clearly, we can say that thanks to the normalization annealing after the first, second and third pass we obtain values of R_e, R_m, and elongation A_5 almost identical to condition after rolling + normalizing. We can therefore conclude that after the normalization a dislocation annihilation process takes place, thus removing dislocation strengthening at all. Of course, this conclusion is not rock-solid as it assumes no change in ferritic grain size as well as pearlitic volume ratio. Our initial metallographic analyzes confirmed this fact, as presented in Table 7.

Table 6 Mechanical properties of cold drawn tubes

Sample	O.D. (mm)	W.T. (mm)	Condition	R_p 0,2 (MPa)	R_m (MPa)	$A_{5,6}$ (%)
A1	33,7	2,6	Rolled	338	406	45,9
A2	33,7	2,6	Rolled + normalized	285	391	41,1
ZB3	28	2,15	1st pass + normalized	313	395	32,8
ZC3	22,85	1,725	2nd pass + normalized	311	398	31
ZD3	18	1,475	3rd pass + normalized	341	407	34,2

Table 7 Ferritic grain size for individual conditions states after normalization

Condition	**Average ferritic grain size d_{str} (μm)**
1st pass + normalized	16,1
2nd pass + normalized	15,6
3rd pass + normalized	12,2

After normalization all samples enjoyed a proper elimination of deformation structure. The resulting microstructure is characterized by polyhedral ferritic grains, while in terms of direction (transverse – longitudinal) we did not witness significant differences in the microstructure. Please note the growth of ferritic grains in the outer and inner surface of the tubes. These domains exhibit some decarburization.

The precision tubes obtained can now be used in subsequent hydroforming process, producing vital parts especially for automotive industry [4].

CONCLUSIONS

In this paper, mechanical properties of steel tubes after several technological steps during the 3-pass cold drawing process in Železiarne Podbrezová have been investigated experimentally. Also, pilot analyses and assessments have been made as well. Results obtained suggest that the simple mechanical tensile tests cannot be directly implemented for limiting drawing states assessment. This is caused by the different stress state in comparison with the actual stresses occurring in cold drawing.

ACKNOWLEDGEMENT

This paper shows intermediate results from Research Project 3/2014/ŽPVVC „TUMIFORM – Optimization of precision tube drawing technology considering dislocation theory, microstructure, and plasticity limit“, currently being solved at ŽP Research and Development Centre in Podbrezová, Slovakia.

REFERENCES

[1] Parilák, Ľ. a kol.: Structural prediction of mechanical properties of HSLA steels, Microalloyed HSLA steels. Proceedings of Microalloying 1988. Chicago, USA, 24. 30. 1988, pp. 559 – 569

[2] Parilák, Ľ., Mojžiš, M., a kol.: Mikroštruktúrne aspekty tvárnenia za studena pri ťahaní presných rúr, VS 24/2013/ŽPVVC, 10.12.2013

[3] RIDZOŇ, M.: *The Effect of Technological Parameters Influencing the Properties of Seamless Cold-Drawn Tubes*, 1st ed. (Scientific monographs) Köthen: Hochschule Anhalt, 2012, 89 pp. ISBN 978-3-86011-048-5

[4] CECLAN, V. et al.: *Quality of the hydroformed tubular parts*. Advanced Engineering Forum 8, pp 215 – 224